DEVELOPMENT OF IRON OXIDE-RICH GLASS-CERAMIC FRITS AND GLAZES FOR APPLICATION ON PORCELAIN FLOOR TILES

(1) Gustavo Rosales, (2) Juan B Carda Castelló, (1) Thierry Poirier,
(3) José Pascual Cosp, (1) Joaquín Lira Olivares

(1) Department of Materials Science, Universidad Simón Bolívar,
Caracas, VENEZUELA.
(2) Department of Organic and Inorganic Chemistry, Universidad Jaume I,
Castellón, SPAIN.
(3) Department of Civil Engineering, Materials and Manufacturing,
Universidad de Málaga, Malaga, SPAIN.

ABSTRACT

In this study, different frit compositions were prepared in the system SiO_2-CaO-Fe_2O_3, keeping the SiO_2:CaO ratio constant and following the wollastonite ($CaSiO_3$) stoichiometry. At the same time, the amounts of Fe_2O_3 were varied between 10% and 40% by weight. The frits were melted in an industrial pilot kiln at 1500°C and characterised using several different techniques in order to study the crystalline character of the frits and glazes and to assess their suitability for floor and wall tile production processes. The microstructure of the frits analysed with SEM revealed the presence of magnetite in the sample with 40% Fe_2O_3, which was the only sample with a glass-ceramic character; nevertheless, XPS and TEM tests revealed the possible presence of crystals in the form of Fe0, FeO, Fe_2O_3 and Fe_3O_4 in all the samples, even though the XRD tests displayed a predominantly glassy character. Finally, in order to confirm appropriate glaze maturing, glaze slips were prepared and the glaze applied to porcelain tile bases. The glazes treated at 1200°C displayed a glass-ceramic character with parawollastonite crystals in the samples with 10% and 20% of Fe_2O_3 and cristobalite and hematite (α-Fe_2O_3)

crystals in the samples with 30% and 40% iron oxide. It is important to note that the fast heating rates of the firing kilns prevented the development of certain phases and defects in the glazes encountered on a laboratory scale. In the future, it is hoped that a method can be designed based on varying the manufacturing parameters to enable the development of semi-conducting glaze compositions for use in anti-static glazes. Semi-conduction is currently inhibited by the oxidising atmosphere present in conventional firing kilns in the ceramic industry. The glazes displayed good adaptability to porcelain tile bases with defect-free surfaces.

1. INTRODUCTION

Glass-ceramic glazes for floor and wall tiles have been of great importance to the ceramic industry thanks to the advantageous properties they offer, such as high resistance to wear or to chemical corrosion, toughness, or ability to adapt to polishing process. Their technical and aesthetic attributes generally tend to exceed those of their glassy counterparts. [1,2,3]

Numerous properties have been developed by modifying the chemical components and microstructure through the nucleation of crystals in the glass. Examples of innovation in frit and glaze production include the creation of characteristics such as heating, bactericidal, non-slip or anti-static properties [4].

The chemical system SiO_2-CaO-Fe_2O_3 has demonstrated in numerous studies its capacity to vitrify and form eutectic mixtures at high temperatures and to crystallise phases such as pseudo-wollastonite, magnetite and hematite in subsequent heat treatments involving nucleation and crystallisation. Among the most interesting properties obtained using these systems is ferrimagnetism, a product of the crystallisation of magnetite, with applications in cancer-fighting treatments such as hyperthermia.[5] Similarly, the development of semi-conductor properties using microstructures based on wollastonite, hematite and silica-rich glass is still a subject of study [6]. It is well known that electricity conduction in glasses rich in iron oxide and in crystalline phases such as magnetite is due to the simultaneous presence of Fe^{+2} and Fe^{+3} valences as a result of a mechanism known as polaron hopping [7]. This system enables anti-static and/or heat-emitting glazes to be manufactured. Prior to this, anti-static glazes had been successfully developed using the SnO_2-Sb system[4]. Furthermore, these glass-ceramics can be used as aggregate in concrete to absorb high-intensity electromagnetic waves [8].

This paper studies the feasibility of developing iron oxide-rich frits and glazes in the system SiO_2-CaO-Fe_2O_3 for porcelain floor tiles, when subjected to industrial firing processes.

In this sense, our studies have focused on the feasibility of forming glass frits with the purpose of controlling crystallisation during subsequent heat treatments.

It should be noted that the heating kinetics of a laboratory kiln differ greatly from an industrial scale kiln, which may have an effect on nucleation and crystallisation in glazes, thereby reducing the degree of crystallisation in certain cases [9]. The use of TiO_2 as a nucleating agent in the SiO_2-CaO-Fe_2O_3 system has also been studied, but has not been found to have a significant effect on the kinetics of the devitrifying process.[6]

The studied compositions (see figure 1) were designed to obtain a weight ratio of SiO_2-CaO of 1.5-2, which would provide pseudo-wollastonite as some of the crystalline phases. On the basis of this ratio, the percentages of Fe_2O_3 were increased to 10, 20, 30 and 40% by weight. With its needle-like shape, pseudo-wollastonite generally increases wear and scratch resistance, and provides the surface with a pleasant opacity [10].

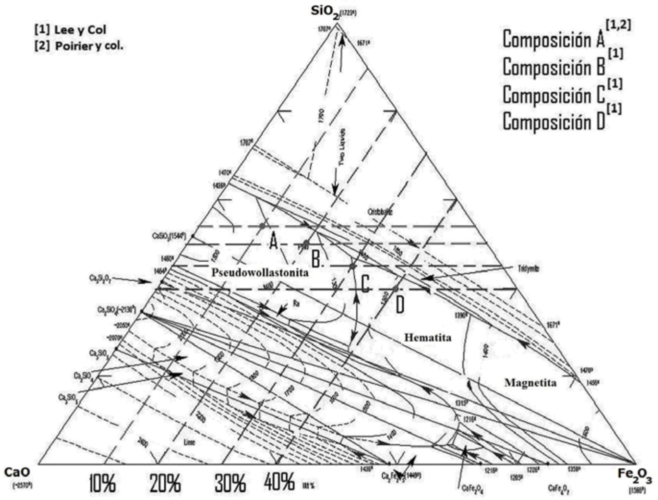

Figure 1. Equilibrium phase diagram for the SiO_2-CaO-Fe_2O_3 system, showing the compositions studied in percentage by weight [6,11,12].

Compositions A and B are closest to the equilibrium area for pseudo-wollastonite, whereas compositions B and C are nearer the equilibrium area for hematite. Compositions C and D may tend to form magnetite crystals during crystallisation.

For the purposes of studying the development of glass-ceramic frits and glazes adapted to cycles of porcelain bodies that may develop ferrimagnetic or semi-conducting properties, the following objectives were set:

- To develop iron oxide-rich frits and to assess their glassy character using different techniques to monitor their subsequent crystallisation; and
- To use the developed frits to formulate glass-ceramic glazes with technical properties suitable for subsequent porcelaining cycles and characterisation.

2. EXPERIMENTAL

2.1. Materials and methods.

2.1.1. Raw materials and compositions used in this study.

Industrially available raw materials were used for the purposes of this study, the specification of which all meet our standard quality parameters. Table 1 lists the raw materials and theoretical compositions studied.

Raw material	Purity	Particle size
SiO_2	99%	35% residuo tamiz 40 μm
$CaCO_3$	99,2%	5-12 μm
Fe_2O_3	95%	0,30% residuo tamiz 44 μm

Sample	SiO_2	CaO	Fe_2O_3
A	55	35	10
B	50	30	20
C	45	25	30
D	40	20	40

Table 1. Industrial raw materials used for the studied frits and compositions.

2.1.2. Methodology for obtaining glass-ceramic frits and glazes.

The frits were obtained in a natural gas-fired industrial testing kiln at a maximum temperature of 1450 °C for 2 hours before being quenched in water.

The glass-ceramic glazes were obtained by mixing these frits ground to an average size of 10 µm with CMC, sodium tripolyphosphate (STPP), kaolin and sufficient water to generate a glaze slip. The glaze was applied on to the porcelain stoneware body and then fired in a porcelain tile thermal cycle. The glazes were subjected to heat treatment at 1200 ºC, the same as for porcelain tile, in an industrial furnace.

2.2. Characterisation techniques used.

X-ray diffraction (XRD). The equipment used to characterise the frits and glazes was a Bruker AXS D4 ENDEAVOR diffractometer with a copper anode. Readings were taken at an intensity of 20 mA, a voltage of 40KV and a 2θ range from 10 to 70°. Scanning speed was 0.005°/s.

X-ray fluorescence (XRF). This technology was used for chemical analysis of the resulting frits using a Bruker AXS S4 Pioneer XRF unit.

Scanning electron microscopy-energy dispersive spectroscopy (SEM-EDS). This was used for the microstructural and chemical characterisation of the frits and glazes. A LEO 440i SEM model was employed in these tests, using a back-scattered electron detector and a secondary electron detector, with a voltage of 20kV and 2000 and 100 pA respectively. Oxford Link ISIS was used for the EDX micro-analysis.

X-ray photo-electron spectroscopy (XPS) and transmission electron microscopy (TEM). These two tests respectively enabled the surfaces and the crystallinity of the frits to be characterised. For the XPS tests, a Physical Electronics ESCA 5701 system was used, while for the TEM tests, a Phillips CM-100 was used. These particular tests were carried out thanks to the collaboration of the Department of Civil Engineering, Materials and Construction at the University of Malaga (Spain).

Hot stage microscopy. This technique was used to determine the characteristic temperatures of each frit. A *Misura* 3.32 hot stage microscope was used with a thermal cycle between 600 °C and 1400 °C, at a heating rate of 20°C per minute.

Differential dilatometry. A Bahr Thermo-analyse DIL80IL was used for the differential dilatometry testing. The program employed for all cycles consisted of a heating rate of 5ºC per minute from 25°C to 1250°C. The dilatometric coefficients were taken for each frit using Appen's formula simply for use as a comparison [13].

3. RESULTS AND DISCUSSION

3.1. Frit characterisation.

3.1.1. Chemical analysis of the frits.

Table 2 below shows the XRF chemical analysis on the resulting frits.

Sample	SiO_2	CaO	Fe_2O_3	Al_2O_3	Na_2O	MgO	K_2O
A	52.70	31.00	8.10	3.20	0.20	0.40	0.50
B	49.30	27.40	19.00	2.10	0.90	0.10	0.10
C	44.80	24.00	23.60	4.00	0.10	0.20	0.30
D	39.20	19.00	33.50	5.10	<0.05	0.10	0.20

Table 2. XRF chemical analysis of the frits obtained.

Significant deviation is observed from the theoretical composition values for all frits due to the preferential introduction of alumina, possibly from the melting crucibles, caused by an increase in Fe_2O_3 in the various samples and increased Al_2O_3 solubility in the molten mass. This is indicative of the extremely corrosive nature of these chemical systems at high temperatures in the presence of alumina. Furthermore, one can also see that the SiO_2/CaO ratio remains approximately within the pseudo-wollastonite range (1.7-2).

3.1.2. XRD crystallinity analysis.

The XRD diffractograms of frits A, B, C and D are shown below in figure 2.

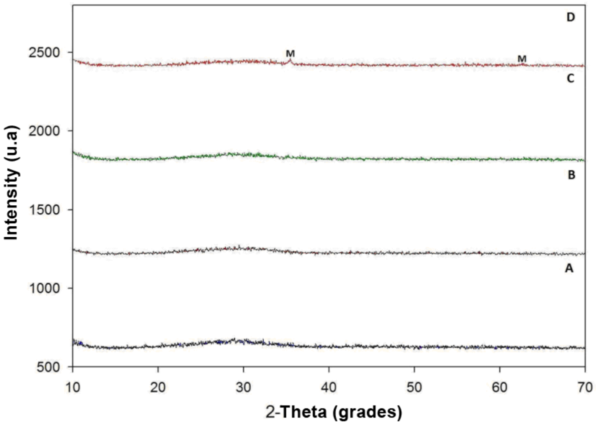

Figure 2. XRD diffractograms of the frits under study. M-Magnetite-740748.

As can be seen in the above graph, the diffractograms generally reveal the frits to have an amorphous nature. However, composition D does display small peaks of crystallinity that are possibly associated with magnetite that, according to the results of the diffraction tests, is not fully crystalline [14].

3.1.3. SEM study of crystallinity.

In the SEM studies (figure 3), composition D clearly reveals the presence of crystalline phases with a dendrite structure typical of magnetite in iron oxide-rich glass where crystallisation during cooling leads to the formation of these structures. The other samples (A-B-C) appeared to display a glassy nature because of the homogeneity of their surfaces. The EDX patterns revealed homogenous compositions that resembled each of the experimental compositions.

Generally, magnetite crystallisation in these glasses is enhanced when, during cooling, iron immiscibility occurs in the melt. This, in terms of thermodynamics, causes the precipitation of iron-based crystalline phase nuclei with dendrite morphologies, typical of strong undercooling [15]. The magnetism observed in frits C and D corroborate the observations made in figure 2.

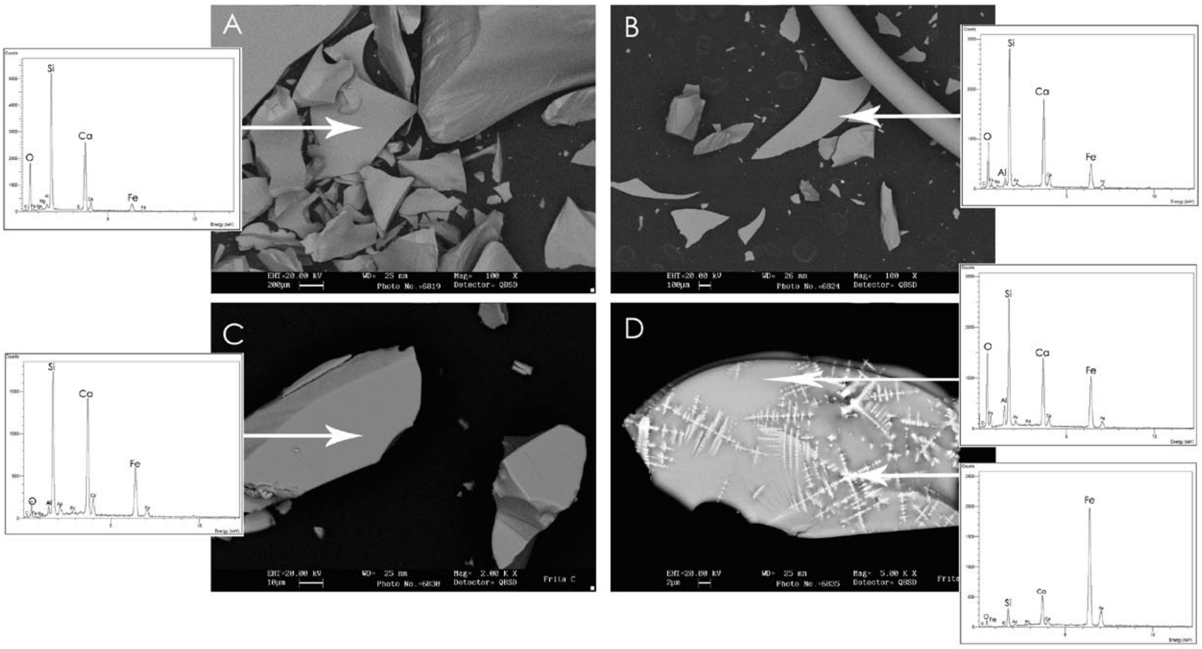

Figure 3. SEM images of studied frits, in the back-scattered electron mode.

3.1.4. TEM study of crystallinity.

Preliminary tests, not presented in this paper, indicated a predominantly amorphous glass with a similar composition to the formulated compositions. However, a semi-crystalline character was detected in several particles in the frits (figure 4). As can be seen in the foregoing figure, the material is predominantly amorphous, although in samples A, B and D, one can observe a slightly crystalline character, confirmed by the ring patterns. EDS chemical analysis of samples A and B reveal a high percentage of Al and O, which could be associated with the presence of alumina from the melting crucibles. Furthermore, in samples C and D (which are richer in Fe_2O_3), small crystals (possibly magnetite) can be observed, though the crystalline nature of C is not so visible in samples A, B or D. The high iron content in the EDS analysis of samples C and D and the difference in the ring patterns in relation to samples A and B lead one to suspect the presence of magnetite. It is important to bear in mind that samples C and D were tested magnetically with a common magnet and both responded to the magnetic field, the response being stronger in composition D.

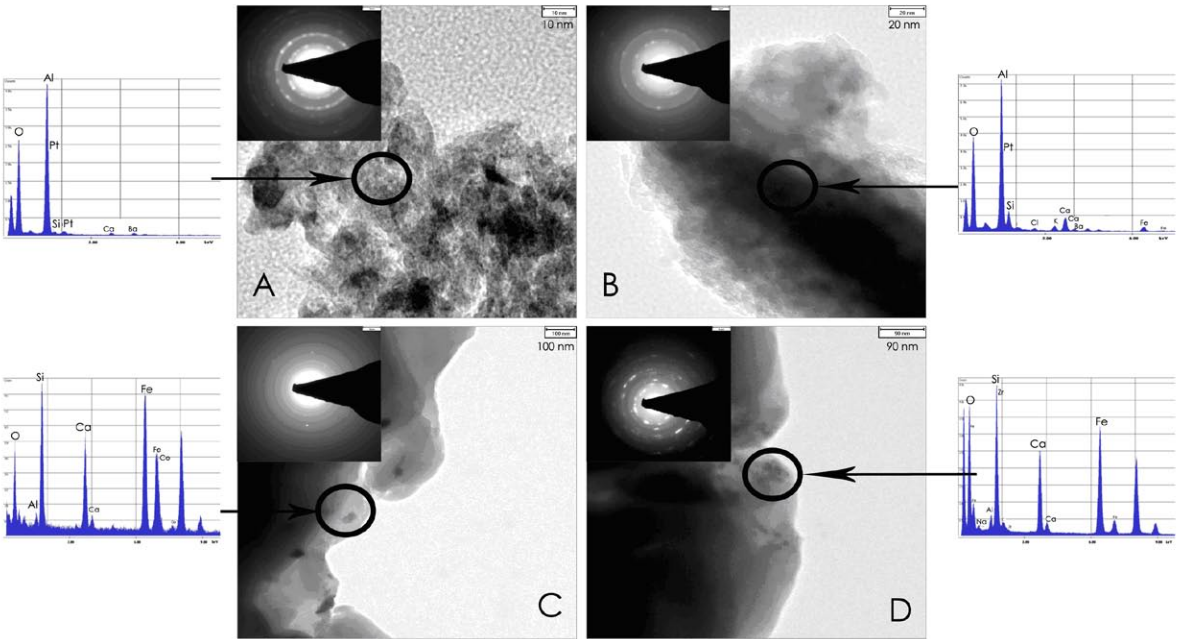

Figure 4. TEM imaging, EDS patterns and electron diffraction patterns for the frits being studied.

3.1.5. Surface characterization of the frits using XPS.

XPS is a surface spectroscopy technique that enables one to determine how the atoms in the surface are bonded together, so that it can provide additional data for the study of crystallinity in this type of glass. Generally, the Fe^{+n} ions in glass sensitive to the atmosphere tend to form iron oxides at the surface when subjected to the presence of oxygen and high temperature. Figure 5 below shows the deconvolutions of the $Fe2p_{3/2}$ XPS spectrum for three compositions (A-B-D) [7].

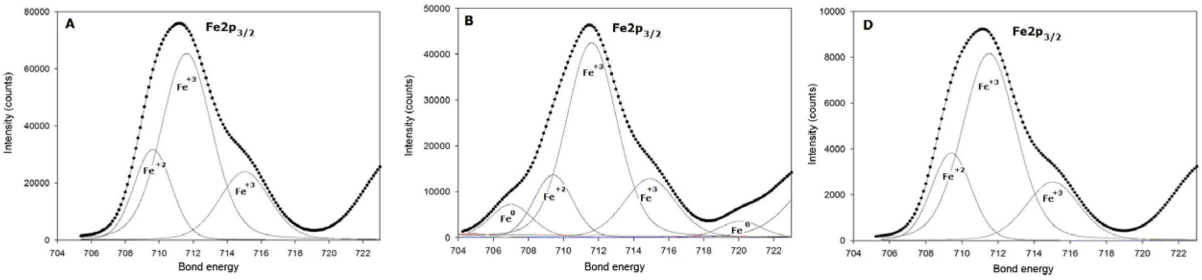

Figure 5. Deconvolution of Fe2p3/2 XPS spectra for compositions A, B and D.

The above figure shows that all the compositions, except B (which contains Fe^0), display Fe^{+2}, which corresponds to 709.6 eV, characteristic of FeO, possibly Fe^{+3}, corresponding to 711-711.2 eV, possibly in a state affected by the coordination environment, and Fe_2O_3 and Fe_3O_4 (Fe^{+3} in Fe_2O_3/Fe_3O_4 environment), which corresponds to 715.03 eV. The Fe^0 corresponds to lines 707 eV and 720.1 eV, characteristic of metal iron.

One of the most significant observations in this spectrum is the possible presence of Fe^0, FeO, Fe_2O_3 and Fe_3O_4 surface crystalline phases, which generally affect crystallisation in iron oxide-rich glasses. Although the XRD spectra do not reveal the presence of such crystal phases, the results of the TEM, electron diffraction and XPS tests all appear to confirm their presence, albeit incipient, in the initial frits. This confirms that, even with low Fe_2O_3 content and high quenching speeds, the crystallisation of iron oxides is inevitable. This has been verified in numerous papers by Kamaranov et al [14].

3.1.6. Dilatometry and hot stage microscopy testing of the frits obtained.

Table 3 below provides a summary of the dilatometric properties of the studied glasses.

Characteristic points			**α($10^{-7}K^{-1}$)(1)**		**α($10^{-7}K^{-1}$) (2)**
Sample	T_g (°C)	T_a (°C)	50-300°C	300-500°C	20-400°C
A	713	787	78.2	79.7	72.8
B	657	1044	73.6	77.8	73.0
C	791	1121	72.1	79.7	58.5
D	742	1090	85.6	87.4	63.9

Table 3. Characteristic points (T_g-glass transition temperature and Ta- dilatometric softening temperature) and linear dilatometric coefficients for the studied frits (1). Linear dilatometric coefficients calculated with the Appen formula (2).

The above table shows that in samples A and B, transition temperature Tg tends to decrease as Fe_2O_3 is increased. This is understandable bearing in mind that in silicate glasses, the Fe^{+3} is generally inserted into the glass partly in octahedral coordination (modifying oxide), which reduces glass refractoriness. However, at 30% Fe_2O_3, glass refractoriness increases, which does not match the trend observed in samples A and B. The possible presence of crystalline phases in C and D may delay the glassy transformation of the glasses. This same phenomenon is observed with the glass softening temperature. On the other hand, the linear dilatometric coefficients determined between 50º to 300°C and 50º to 500°C are similar and lie in the ranges of 73.6-85.6x10^{-7} K^{-1} and 77.8-87.4^{-7} K, respectively. These values are generally high for use in porcelain glazes (70x10^{-7} K^{-1}); however, in the future the composition could be altered to reduce thermal expansion and thus prevent stresses between the glaze and the base material. It should be noted that the theoretical Appen values were similar in compositions A and B and differed significantly in compositions C and D, where the crystal content is presumably higher. Similar variations in theoretical thermal expansion coefficients in the presence of crystalline phases have been previously reported.[16]

Figure 6 below shows the sintering curves and softening, melting and sintering points determined by hot-stage microscopy for frits A, B and D.

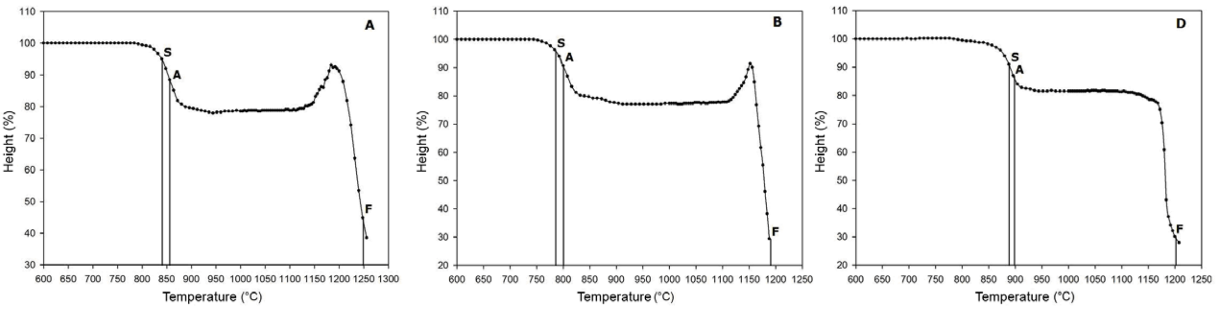

Figure 6. Sintering (S), softening (A), and melting (F) points for samples A, B and D determined by hot stage microscopy. Half-sphere (ME) and sphere (E) points could not be calculated as they could not be observed.

In all compositions, melting occurs at approximately 1200 °C. Furthermore, sintering is achieved at approximately 850 °C in all compositions, though it is later in sample D, with a sintering point of nearly 900 °C, as a result of the possible crystallinity of the sample. The significant expansion noted in A and B (also observed in C) at around 1150 °C is due to the possible reduction of Fe_2O_3 type iron oxides nucleated during heat treatment and the release of O_2 in the frit. In glass D, no such expansion is observed at 1150°C, which may be due to a low Fe^{+2} concentration, which may be combined with the magnetite or strongly bonded to the glassy network, thereby restricting the formation of Fe_2O_3. It should be noted that in iron oxide-rich glasses, the Fe^{+2} ions tend to oxidise superficially and switch to an Fe^{3+} state, which may be the cause of the effects observed in samples A, B and C. Laboratory tests revealed the presence of surface pinholes in samples A, B and C, which is in line with the results observed.

3.2. Characterization of the glazes obtained.

3.2.1. XRD crystalline study of the glazes.

The XRD spectra and the SEM surface imaging of the glazes obtained are shown in figure 7.

As can be seen from the illustration, the glazes are able to develop a glass-ceramic character after being subjected to industrial firing cycles. In glaze A, the predominant phase is parawollastonite, which is to be expected from a thermodynamics point of view on the basis of the phase diagram for this system (figure 1). Moreover, in glaze B, no crystalline phases can be observed, which would seem to indicate that the increase in the quantity of Fe_2O_3 prevents crystallisation of the parawollastonite in such firing cycles. Finally, in glazes C and D, the presence of hematite is observed as the predominant phase. This concurs with the predictions of the phase diagram (figure 1) and with the fact that in iron oxide-rich glass powders, the predominant surface phase is hematite when heating is carried out in air [14, 15].

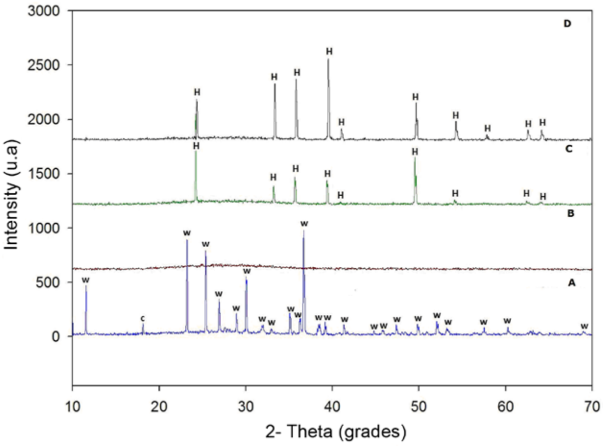

Figure 7. XRD surface spectra of the glass-ceramic glazes obtained on porcelain stoneware. W. Parawollastonite 760925, C. Cristobalite 790940, H. Hematite 79094.

3.2.2. SEM microstructure study of the resulting glazes.

The surfaces and cross-sections of glazes A and D may be observed in figure 8. The SEM images for glazes B and C indicated surface properties similar to those of A and D, respectively, and were therefore omitted from this work.

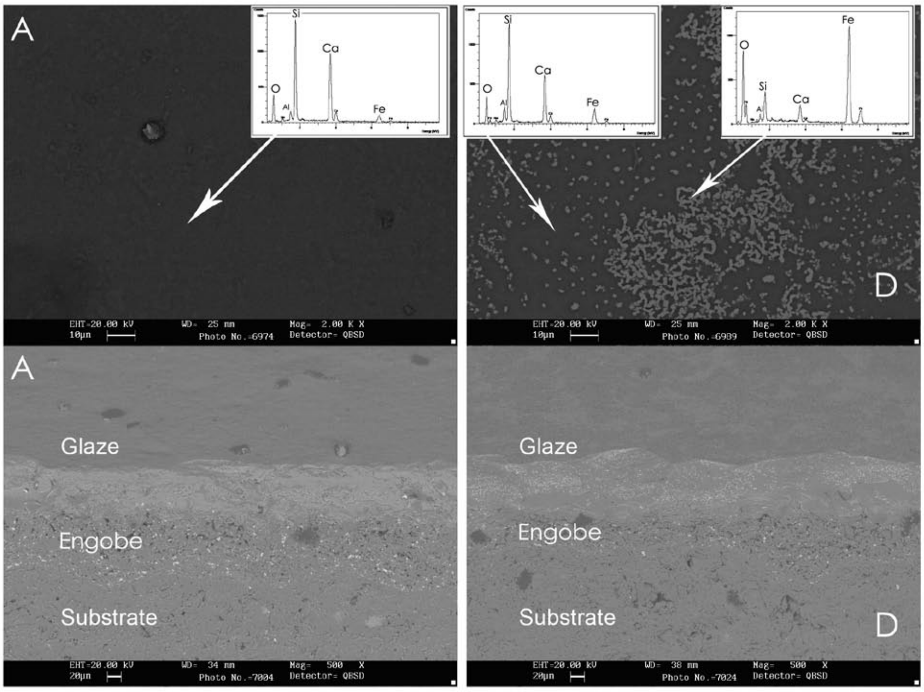

Figure 8. Back-scattered electron SEM imaging and EDS spectra at the surface and cross-section for glazes A and D.

Parawollastonite crystals were not observed with back-scattered electron scanning of glaze A (figure 8). However, the crystals may merge with the substrate due to the compositional similarity with the glass, bearing in mind that the iron content is low (see EDS spectrum). The cross-section of sample A exhibits good bonding with the engobe and the substrate, with no closed porosity, chipping or cracking. On the other hand, in sample D, numerous Fe_2O_3 crystals are observed as the XRD and EDS spectra show. The absence of pinholes or defects, which was to be expected in view of the sintering curves obtained by hot stage microscopy, indicates that the high speed of the firing cycles could delay the reduction of hematite and thus prevent such surface defects. Furthermore, it is important to note that these industrial firing cycles were carried out at a heating rate of approximately 150 °C/min, which prevents hematite decomposition in the frits, as observed in the hot stage microscopy curves taken at 20°C/min. Finally, the cross-section of composition D appears free of defects, like in glaze A. These crystalline phase-rich glazes could justify greater toughness.

4. CONCLUSIONS

- Compositions were formulated in the system SiO_2-CaO-Fe_2O_3, which displayed a predominantly glassy character, with an incipient presence of magnetite and possibly other iron oxides.
- The characterisation of the developed glasses demonstrated that, even at high quenching speeds in the frit-making process, the formation of iron-rich crystalline phases in these systems cannot be prevented.
- The fired coatings, applied as glaze compositions, exhibit good industrial adaptability, homogeneity, and ability to develop crystalline phases and defect-free surfaces.
- The developed glazes open up new prospects for the future development of iron oxide-based glazes with anti-static properties.

ACKNOWLEDGEMENTS

The authors wish to express their gratitude to all the members of the Servei Central d´Instrumentació científica at Jaume I University in Castellón, to the Department of Civil Engineering, Materials and Manufacturing at the University of Malaga for performing many of the characterisation tests, and to the Surface Engineering Department at the Simon Bolivar University, Venezuela, for their support throughout this project.

REFERENCES

[1] M. TICHELL, E. FONTANET, A. PASCUAL, J. BAKALIi, G. MONRÓS, P. ESCRIBANO, J.B. CARDA,: "Estudio del desarrollo de aplicación de esmaltes de naturaleza vitrocristalina en orden a mejorar las propiedades tecnológicas de los esmaltes convencionales", QUALICER 1996, P.GI, 209-238.

[2] E. QUINTEIRO, A. ORTEGA BOSCHI, C. LEONELLI, T. MANFREDINI, C. SILIGARDI,: "Sistemas vitrocerámicos compatibles con las condiciones de cocción utilizadas en la industria cerámica", QUALICER 2002, P.GI, 301-311.

[3] J. MARTINEZ, M. ARIÑO, I.T. MARINOVA, M.C. PEIRÓ, I. NUÑEZ, J.B CARDA,: "Desarrollo de nuevos esmaltes para soportes de gres y gres porcelánico adaptado a los procesos de pulido y que representan buenas prestaciones técnicas y estéticas", QUALICER 2004, P.GI, 137-152.

[4] J. NUÑEZ, J.M. PEDRA, M.PEIRÓ, J.J GÓMEZ, L. CHIVA, J.B. CARDA,: "Investigaciones de interés industrial sobre baldosas cerámicas", Cerámica Industrial, Vol. 252, 2002.

[5] Y. EBISAWA, Y. SUGIMOTO, T. HAYASHI, T. KOKUBO, K. OHURA, T. YAMAMURO,: "Crystallization of (FeO, Fe_2O_3)-CaO-SiO_2 Glasses and Magnetic Properties of their crystallized products", Nippon Seramikkusu Kyokai Gakujutsu Rombunshi ,Vol. 99 , 1991.

[6] T. POIRIER, N. LABRADOR, M.A. ALVAREZ, C. LAVELLE, N. ENET, J. LIRA-OLIVARES,: "Formation of crystalline phases in (SiO_2–CaO–Fe_2O_3)–TiO_2 based glasses", Materials letters, Vol. 59, 308–312, 2005.

[7] A. MEKKI, D. HOLLAND, C.F. MCCONVILLE, M. SALIM,: "An XPS study of iron sodium silicate glass surfaces", Journal of non-Crystalline Solids, Vol. 208, 267-276, 1996.

[8] A.A. FRANCIS,: "Crystallization kinetics of magnetic glass–ceramics prepared by the processing of waste materials", Materials Research Bulletin, Vol. 41, 1146–1154,2006.

[9] L. FROBERG, T. KRONBERG, L. HUPPA, M. HUPPA,: "Influence of firing parameters on phase composition of raw glazes", Journal of the European Ceramic Society, Vol. 27, pp. 1671–1675, 2007.

[10] L. SANCHEZ-MUÑOZ, J.B. CARDA CASTELLÓ,; "Enciclopedia Cerámica-Materias Primas y Aditivos", Vol. 2.2, Faenza Editrice, (2003).

[11] L. YONG. K, C. SE. Y,: "Crystallization and Properties of Fe_2O_3-CaO-SiO_2 glasses", Journal of The American Ceramic Society, Vol. 79, 1995.

[12] THE AMERICAN CERAMICS SOCIETY,: "Acers-NIST Phase Equilibria Diagrams", NIST Standard Reference, Version 3.1, 2004-2005.

[13] E. BOU, M.F. GAZULLA, M.J. ORTS, E. SANCHEZ, V. SANZ, F. VICIANO, "Manual para el control de calidad de materias primas empleadas en la preparación de los vidria-

dos cerámicos", Procedimiento E18, Instituto de Tecnología Cerámica (ITC), Castellón, España, (2000).

[14] A. KAMARANOV, M. PELINO, "Crystallization phenomena in iron-rich glasses", Journal of non-Crystalline Solids, pp. 139-151, 2001.

[15] A. KARAMANOV, P. PISCIELLA, M. PELINO, "The crystallisation kinetics of iron rich glass in different atmospheres", Journal of the European Ceramic Society, Vol 20, pp. 2233-2237, 2000.

[16] M.G. RASTEIRO, T. GASSMAN, R. SANTOS, E. ANTUNES, "Crystalline phase characterization of glass-ceramic glazes", Ceramics International, Vol 33, 345–354, 2007.